Principle and Control Design of a Novel Hybrid Arc Suppression Device in Distribution Networks

Bishuang Fan, *Member, IEEE*, Ganzhou Yao, *Student Member, IEEE*, Wen Wang, *Member, IEEE*, Xiangjun Zeng, *Senior Member, IEEE*, Josep M. Guerrero, *Fellow, IEEE*, Kun Yu, *Member, IEEE*, and Chao Zhuo

***Abstract*—A single line-to-ground (SLG) fault may lead to a more severe line-to-line fault and power supply interruption if the ground-fault current exceeds a certain value. Arc suppression device (ASD) is a good solution to eliminate the ground-fault current. A novel hybrid ASD is proposed in this article, which consists of a passive device and an active one. The passive device utilizes multiterminal breakers and an isolation transformer to couple a secondary voltage of a zig-zag grounding transformer to the neutral point to compensate the majority of the ground-fault current. The active device uses a single-phase voltage source inverter to eliminate the residual fault current due to the leakage inductance of the zig-zag grounding transformer in the passive device. A dual-loop voltage and current control method for the active device is designed for the accurate residual current compensation. Results of simulation and prototype experiment validate the effectiveness of the proposed hybrid ASD. The proposed hybrid ASD does not need to detect distributed line-to-ground parameters, and it has lower cost, less control complexity, higher reliability, and better performance, compared to other ASDs.**

***Index Terms*—Distribution networks, dual-loop control, hybrid arc suppression, single line-to-ground (SLG) fault.**

I. Introduction

RELIABLE power supply is of great significance in distribution networks [1]. To enhance the reliability, a neutral noneffectively grounded distribution system is usually allowed to maintain power supply for about 1 h before a single line-to-ground fault (SLG) is isolated. However, if the fault current exceeds a certain value, the fault-induced arcs may not self-extinguish, resulting in arc overvoltage and insulation damage. In this way, a tolerable SLG fault could lead to more severe line-to-line faults and power supply interruptions eventually [2], [3]. Therefore, it is highly desirable to extinguish fault-induced arcs when a SLG fault occurs [4], [5].

The existing arc-suppression methods can be divided into two categories: current-based compensation and voltage-based compensation. One typical current-based compensation method is to earth the system neutral through an arc suppression coil (ASC) [6]–[8]. The ASC can suppress arcs by injecting an inductive current to compensate the capacitive fault current, so that nonpermanent SLG faults can be self-extinguished without breakers operations. However, the ASC with fixed parameters is difficult to fully compensate the capacitive current (lead to series resonance otherwise), active power, and harmonic current. Another current-based compensation method is to earth the system neutral through a current-type inverter, which is able to adjust the injected inductive current based on the measured capacitive current [9]–[11]. Nevertheless, it is difficult to accurately measure the capacitive current in distribution networks, especially under an SLG fault condition [12].

The voltage-type arc-suppression methods are also proposed in literature [13]–[15]. The ground-fault transfer device can automatically compensate the ASC by quickly grounding the fault phase [14]. However, it relies on accurate faulty phase selection to prevent line-to-line fault. Moreover, its cost is very high when applying to medium-voltage distribution networks. Recently, voltage-source type single-phase inverter is proposed to control the neutral-to-ground voltage to the opposite of the faulty phase voltage. This method does not rely on the distributed parameters and the residual current. Nevertheless, the major shortcoming of the voltage-type inverter-based arc-suppression method is that it requires an electronic device with very large capacity to extinguish the fault-induced arc [16].

Moreover, an additional zig-zag grounding transformer is usually needed to create a neutral point for most medium-voltage distribution networks, which adopt the high-resistance grounding or resonant grounding (RG) method [17]. When an SLG fault occurs, the neutral-to-ground voltage may have phase shift problem in neutral point as the leakage inductance (a zero-sequence impedance) of the zig-zag grounding transformer can build up a neutral voltage shift [18]. This makes it difficult to control the neutral-to-ground voltage to the expected value.

Manuscript received May 28, 2020; revised September 9, 2020 and November 23, 2020; accepted December 21, 2020. Date of publication January 14, 2021; date of current version September 29, 2021. This work was supported in part by the National Natural Science Foundation of China under Award 51877011, 52077010 and 51737002, and in part by the Training Program for Excellent Young Innovators of Changsha under Award kq2009011. *(Corresponding author: Wen Wang.)*

Bishuang Fan, Ganzhou Yao, Wen Wang, Xiangjun Zeng, Kun Yu, and Chao Zhuo are with the Hunan Provincial Key Laboratory of Smart Grids Operation and Control, School of Electrical and Information Engineering, Changsha University of Science and Technology, Changsha 410114, China (e-mail: fanbishuang@qq.com; ygzaddson@126.com; ww_csust@126.com; eexjzeng@qq.com; 1393009168@qq.com; 305661237@qq.com).

Josep M. Guerrero is with the Department of Energy Technology, Aalborg University, 9220 Aalborg, Denmark (e-mail: joz@et.aau.dk).

Color versions of one or more figures in this article are available at https://doi.org/10.1109/TIE.2021.3050390.

Digital Object Identifier 10.1109/TIE.2021.3050390

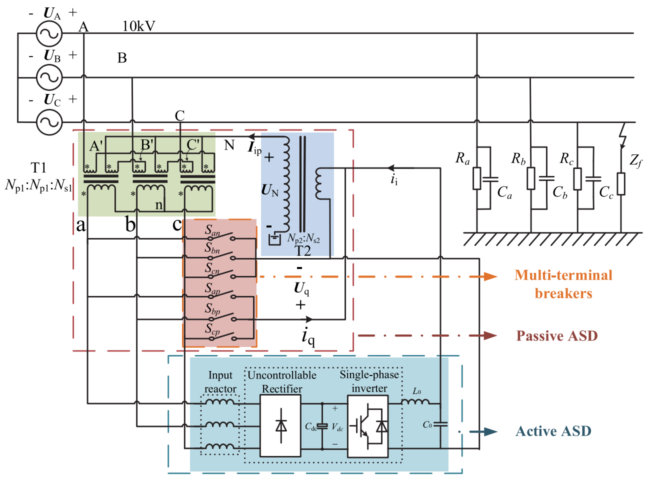

Fig. 1. Sample distribution network with the proposed hybrid ASD.

TABLE I
DISTRIBUTION NETWORK AND ASD VARIABLES

Factor	Note
U_A, U_B, U_C	Three phase positive-sequence voltages
I_A, I_B, I_C	Line-to-line current
R_S, C_S,	Ground resistances, capacitances,
Z_A, Z_B, Z_C	Line-to-ground impedances
$Z_{lk\text{-}T1}$, $Z_{lk\text{-}T2}$	Leakage inductance of T_1, T_2
N_{T2} (N_{p2}: N_{s2})	The turns ratio of the transformer T_2
N_{T1}(N_{p1}: N_{p1}: N_{s1})	The turns ratio of the transformer T_1
$\boldsymbol{U}_{AA'}$ $\boldsymbol{U}_{BB'}$ $\boldsymbol{U}_{CC'}$	Voltages of the primary main windings of T_1
$\boldsymbol{U}_{A'N}$, $\boldsymbol{U}_{B'N}$ $\boldsymbol{U}_{C'N}$	Voltages of the primary side phase-shift windings of T_1
$\boldsymbol{u}_a$ $\boldsymbol{u}_b$ $\boldsymbol{u}_c$	Voltages of the secondary side windings of T_1
$\boldsymbol{U}_F$, $\boldsymbol{I}_F$, Z_F	Ground-fault voltage, current, resistance
$\boldsymbol{u}_q$	Line-to-line voltage generated from T_1
$\boldsymbol{u}_Q$	The voltage $\boldsymbol{u}_q$ considering leakage inductance
$\boldsymbol{U}_N$	Neutral-to-ground voltage
$\boldsymbol{U}_{00}$	Neutral unbalanced voltage
$\boldsymbol{U}_{10}$	The voltage between dot 1 and 0
$\boldsymbol{U}_{ab}$	The voltage between node 'a' and 'b'
$\boldsymbol{U}_{N\_res}$, $\boldsymbol{I}_{res}$	The residual fault voltage and current
$\boldsymbol{I}_{G\Sigma}$	The current flowing through ground impedance
$\boldsymbol{I}_{full\_com}$	The current for full ground-current compensation
$\boldsymbol{I}_{lk}$	The flowing current through leakage of transformers
$\boldsymbol{U}_i$, $\boldsymbol{i}_i$, $\boldsymbol{i}_{i\text{-}asy}$	The output voltage and current of inverter in symmetric and asymmetric system

Thus, the conventional arc-suppression methods are inadequate to increase the neutral-to-ground voltage to the line-to-ground voltage and reduce the residual current to zero at the same time [19]. There is an urgent need in a comprehensive arc suppression device (ASD) that can suppress the ground-fault current under different ground-fault resistances but require less electronic equipment to reduce the cost.

To address the abovementioned issues, a novel hybrid suppression device (ASD) is proposed in this article. The grounding system is composed of a zig-zag grounding transformer, a single-phase isolation transformer, multi terminal breakers, and a voltage source inverter (VSI). The hybrid ASD employs two control algorithms. One is the passive arc-suppression method through the zig-zag grounding transformer for high-power compensation, and the other is the active arc-suppression method through the VSI to eliminate the effect of neutral point phase shift caused by the zig-zag grounding transformer. By regulating inverter's output voltage, the active method can generate the compensated current for the neutral voltage error from phase shift in the neutral point. Together with the passive method, the neutral-to-ground voltage can be controlled to exactly match the opposite of the faulty phase voltage. Meanwhile, the residual fault current can be reduced to near zero to completely distinguish the fault-induced arcs.

The rest of the article is organized as follows. In Section II, the principle of the proposed hybrid ASD is introduced, and VSI-based dual-loop control is presented in Section III. The proposed hybrid ASD is simulated in a typical neutral noneffectively grounded 10 kV distribution network model in MATLAB/Simulink in Section IV. Experiment results on a 10 kV prototype are presented in Section V. Finally, Section VI concludes this article.

II. Principle of Hybrid ASD

A typical neutral noneffectively grounded 10 kV distribution network with the proposed hybrid ASD is illustrated in Fig. 1. The hybrid ASD is comprised of a passive ASD and an active ASD. The passive ASD consists of a zig-zag grounding transformer, a single-phase isolation transformer, and multiterminal breakers. The Zig-Zag grounding transformer (T_1) is used to create the neutral point, while the single-phase isolation transformer (T_2) is utilized to inject a voltage to the neutral point. The secondary sides of the both transformers are connected by multiterminal breakers (S_{an}, S_{bn}, S_{cn}, S_{ap}, S_{bp}, S_{cp}) to select the suitable line-to-line voltage ($\boldsymbol{u}_q$) for the injected neutral voltage. The active ASD consists of an uncontrollable rectifier and a single-phase voltage source inverter. The active ASD is connected to the secondary side of the zig-zag grounding transformer through three input inductors, while connected to the isolation transformer through a LC filter.

The passive ASD is used for high-power compensation, but the leakage inductance of the zig-zag grounding transformer may introduce phase error, resulting in the phase error of the neutral voltage [17]. Meanwhile, as a lower power device, the active ASD can inject the voltage to compensate the phase error of the neutral voltage and the SLG fault residual current. The next two sections will introduce the principles of both the passive ASD and the active ASD. The related variables are summarized in Table I.

A. Principle of Passive ASD

As shown in Fig. 1, the connection type of the zig-zag grounding transformer is Zny11. The phasor relationships among the line-to-line voltages ($\boldsymbol{u}_{ab}$, $\boldsymbol{u}_{bc}$, and $\boldsymbol{u}_{ca}$) and the three-phase positive-sequence voltages ($\boldsymbol{U}_A$, $\boldsymbol{U}_B$, and $\boldsymbol{U}_C$) are presented in Fig. 2. The line-to-line voltage is totally opposite to the associated phase positive-sequence voltage, e.g., $\boldsymbol{u}_{ca}$ and $\boldsymbol{U}_A$, $\boldsymbol{u}_{ab}$, and $\boldsymbol{U}_B$, or $\boldsymbol{u}_{bc}$, and $\boldsymbol{U}_C$. The magnitude relationship in each group depends on the value of turn ratio N_{T1}. The line-to-line

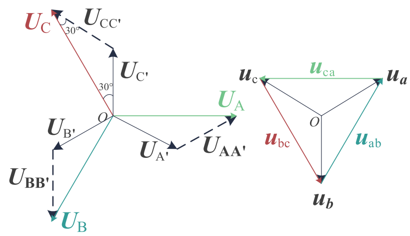

Fig. 2. Voltage phasor diagram of the zig-zag grounding transformer.

voltage $\boldsymbol{u}_{\mathrm{q}}$ can be expressed as below.

$$\boldsymbol{u}_q = \begin{cases} \boldsymbol{u}_{ca} = -\frac{N_{\mathbf{s1}}}{\sqrt{3}N_{\mathbf{p1}}}\boldsymbol{U}_{\mathrm{A}}(S_{\mathbf{an}}, S_{\mathbf{cp}}\ \text{on}) \\ \boldsymbol{u}_{\mathrm{ab}} = -\frac{N_{\mathbf{s1}}}{\sqrt{3}N_{\mathbf{p1}}}\boldsymbol{U}_{\mathrm{B}}(S_{\mathbf{bn}}, S_{\mathbf{ap}}\ \text{on}) \\ \boldsymbol{u}_{bc} = -\frac{N_{\mathbf{s1}}}{\sqrt{3}N_{\mathbf{p1}}}\boldsymbol{U}_{\mathrm{C}}(S_{\mathbf{cn}}, S_{\mathbf{bp}}\ \text{on}) \end{cases}. \tag{1}$$

According to the ideal transformer principle,

$$\boldsymbol{U}_N = N_{T2}\boldsymbol{u}_{\mathrm{q}} = -N_{T2}N_{T1}^{-1}\boldsymbol{U}_{\mathrm{X}}. \tag{2}$$

When ignoring the sign, the neutral-to-ground voltage ($\boldsymbol{U}_{\mathrm{N}}$) can be equivalent to the line-to-line voltage ($\boldsymbol{U}_{\mathrm{X}}$) if the turn ratio number of N_{T2} equals that of N_{T1}, meaning that

$$N_{P2} : N_{S2} = N_{S1} : \sqrt{3}N_{P1} \tag{3}$$

Therefore, if an SLG fault occurs on phases A, B, and C, respectively, we manage to have $\boldsymbol{U}_{\mathrm{N}} = \boldsymbol{u}_{\mathrm{ca}} = -\boldsymbol{U}_{\mathrm{A}}$, $\boldsymbol{U}_{\mathrm{N}} = \boldsymbol{u}_{\mathrm{ab}} = -\boldsymbol{U}_{\mathrm{B}}$ and $\boldsymbol{U}_{\mathrm{N}} = \boldsymbol{u}_{\mathrm{bc}} = -\boldsymbol{U}_{\mathrm{C}}$ within short notice, and that can be expressed as follows:

$$\boldsymbol{U}_N = -\boldsymbol{U}_X. \tag{4}$$

In this way, the passive arc suppression can be achieved for the high-power compensation.

When an SLG fault occurs in phase C, as further arc-suppression needs, a set of breakers S_{bn} and S_{cp} are turned ON to generate the line-to-line voltage $\boldsymbol{u}_{\mathrm{bc}}$ as the input of the secondary-side in the single-phase isolation transformer (T_2), $\boldsymbol{u}_{\mathrm{q}}$. Similarly, if we assume that SLG fault (10 Ω) occurs in phases A and B, respectively, then multiterminal breakers will turn ON the breakers S_{an}, S_{cp}, and the breakers S_{bn}, S_{ap} for generating the correct line-to-line voltage to control the neutral voltage at the neutral point in order to suppress the fault arc.

However, the passive arc suppression is incapable of compensating the phase shift caused by the leakage impedance of transformers and generated during operation process in multi-terminal breakers. In order to solve this problem, the active arc suppression devise is introduced. Thus, if we consider the phase error impact, the leakage impedance of T_1 shall be included in further arc suppression analysis, and $\boldsymbol{u}_{\mathrm{Q}}$ is the isolation transformer secondary-side voltage after considering inductive leakage reactance $Z_{\mathrm{lk\text{-}T1}}$ and $Z_{\mathrm{lk\text{-}T2}}$.

B. Principle of Active ASD

The topology of distribution network in Fig. 1 is converted to the low-voltage side of the isolation transformer and shown in Fig. 3.

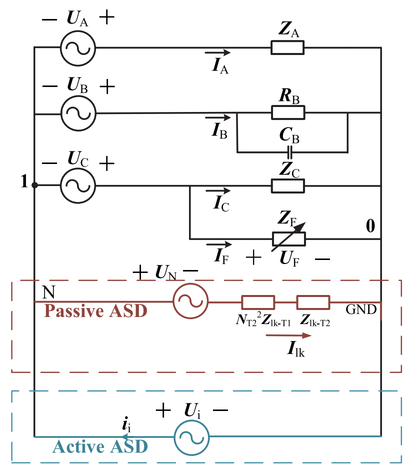

Fig. 3. Simplified distribution network with equivalent passive ASD and active ASD.

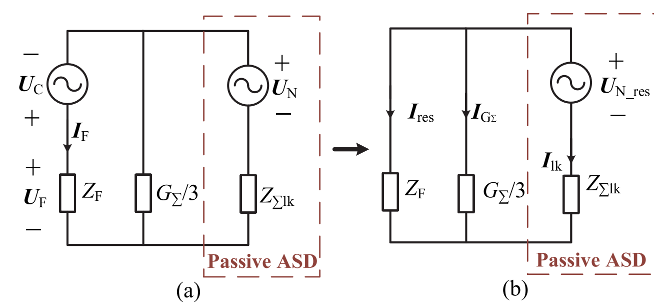

Fig. 4. Zero-sequence circuit of distribution network under an SLG fault. (a) Simplified equivalent circuit before arc suppression. (b) Simplified equivalent circuit with only passive ASD adopted.

According to Kirchhoff voltage law (KVL), we can obtain

$$\boldsymbol{U}_N = N_{T2}\boldsymbol{u}_Q. \tag{5}$$

1) Symmetric Distribution Network: Without loss of generality, it is assumed that an SLG fault occurs on phase C. The zero-sequence circuit of the distribution network with the passive ASD can be represented in Fig. 4. Fig. 4(a) is the simplified distribution network without implementing ASD and Fig. 4(b) adopts passive ASD. G_Σ denotes the impedance of the distribution network and is shown in (6), where Y_{X} is the line-to-ground admittance, i.e., ($X = \mathrm{A}$, B, or C) and ω_0 denotes the fundamental angular frequency.

$$G_\Sigma = Y_\Sigma^{-1} = (Y_A + Y_B + Y_C)^{-1}. \tag{6}$$

Assume SLG fault occurs on phase-C and adopt only the passive ASD with studying in the influence of the leakage impedance of the transformers $Z_{\Sigma\mathrm{lk}} = {N_{\mathrm{T2}}}^2 Z_{\mathrm{lk\text{-}T1}} + 3Z_{\mathrm{lk\text{-}T2}}$, we consider to short-circuit $\boldsymbol{U}_{\mathrm{i}}$ (equivalent as active ASD) above.

Therefore, in Fig. 4(a), according to KVL, we can simply attain the neutral voltage in (7) for successfully eliminating the fault arcs if the fault current is assumed to be equal to zero ($\boldsymbol{I}_{\mathrm{F}} = 0$ and $\boldsymbol{U}_{\mathrm{F}} = 0$),

$$\boldsymbol{U}_{\mathrm{N}} = -\boldsymbol{U}_C\left(1 + 3Z_{\sum lk}G_\Sigma^{-1}\right) \tag{7}$$

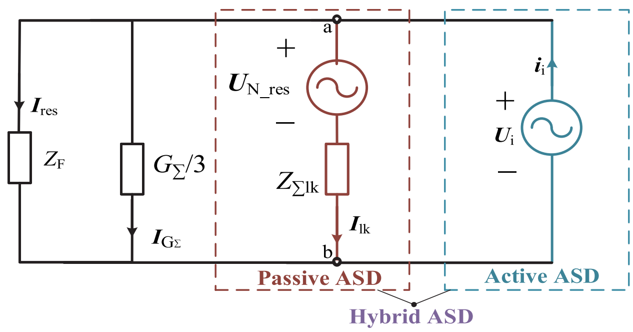

Fig. 5. Zero-sequence circuit of distribution network with adoption in both passive ASD and Active ASD.

That is, by adopt only the passive ASD, the fault current can be constrained down to near zero. But to achieve complete $\boldsymbol{U}_{\text{N}} = -\boldsymbol{U}_{\text{C}}$, we need to further analyze $-3Z_{\Sigma\text{lk}}G_{\Sigma}{}^{-1}\,\boldsymbol{U}_{\text{C}}$, which can be treated as residual voltage of neutral point $\boldsymbol{U}_{\text{N\_res}}$, as shown in (8) and Fig. 4(b). $\boldsymbol{U}_{\text{N\_res}}$ is caused by the phase error of neutral voltage from leakage impedances $Z_{\Sigma\text{lk}}$ exists in transformers.

$$\boldsymbol{U}_{\text{N\_res}} = -3Z_{\sum lk}G_{\Sigma}^{-1}\boldsymbol{U}_{C}. \tag{8}$$

Notice that when the influence of the leakage impedances $Z_{\Sigma\text{lk}}$ is considered, the problem will remain in the passive ASD, making the controlled neutral voltage hard to reach expectation value, Therefore, the exact equation of residual current $\boldsymbol{I}_{\text{res}}$ can be obtained for further ground-fault compensation, by the principle of KVL and voltage divider method.

$$\boldsymbol{I}_{\text{res}} = \frac{-3\boldsymbol{U}_{C}Z_{\sum lk}}{Z_{\sum lk}(G_{\Sigma} + 3Z_{F}) + G_{\Sigma}Z_{F}}. \tag{9}$$

The passive ASD can suppress the fault arc down to certain promised range, leading to the arc condition of not being rekindled. However, it cannot compensate fully the neutral voltage error and residual fault current. Therefore, the low-power active ASD method is co-operated with passive ASD method in Fig. 5, named as hybrid ASD. It constrains the residual fault current down to zero for erasing the neutral voltage error. Then, according to (7), it achieves $\boldsymbol{U}_{\text{N}} = -\boldsymbol{U}_{\text{C}}$.

An equivalent voltage source $\boldsymbol{U}_{\text{i}}$ is treated as the output and the control target of the dual-loop VSI. According to the Kirchhoff theorem, the flowing current $\boldsymbol{I}_{\text{G}\Sigma}$ through the impedance of the distribution network and the flowing current $\boldsymbol{I}_{\text{lk}}$ through the leakage impedances $Z_{\Sigma\text{lk}}$ can be obtain as

For further analysis of active ASD, the only two nodes on Fig. 4(b) is marked for the principle of Nodal-Voltage method, and the voltage between node "a" and "b" $\underline{U}_{\text{ab}}$ can be obtained

$$\boldsymbol{U}_{\text{ab}} = Z_{F}G_{\Sigma}\boldsymbol{U}_{N\_res}(3Z_{F}Z_{\sum lk} + Z_{\sum lk}G_{\Sigma} + Z_{F}G_{\Sigma})^{-1}. \tag{10}$$

According to the Kirchhoff theorem, the flowing current $\boldsymbol{I}_{\text{G}\Sigma}$ through the impedance of the distribution network and the flowing current $\boldsymbol{I}_{\text{lk}}$ through the leakage impedances $Z_{\Sigma\text{lk}}$ can be obtain as

$$\begin{aligned}\boldsymbol{I}_{G\sum} &= 3\frac{\boldsymbol{U}_{\text{ab}}}{G_{\Sigma}}\\ &= 3Z_{F}\boldsymbol{U}_{N\_res}(3Z_{F}Z_{\sum lk} + Z_{\sum lk}G_{\Sigma} + Z_{F}G_{\Sigma})^{-1}\end{aligned} \tag{11}$$

$$\begin{aligned}\boldsymbol{I}_{lk} &= (\boldsymbol{U}_{\text{ab}} - \boldsymbol{U}_{N\_res})Z_{\sum lk}^{-1}\\ &= [Z_{F}G_{\Sigma}(3Z_{F}Z_{\sum lk}^{2} + Z_{\sum lk}^{2}G_{\Sigma}\\ &\quad + Z_{\sum lk}Z_{F}G_{\Sigma})^{-1} - 1]\boldsymbol{U}_{N\_res}.\end{aligned} \tag{12}$$

An equivalent voltage source $\boldsymbol{U}_{\text{i}}$ is treated as the output and the control target of the dual-loop VSI. According to Kirchhoff's current law, the expression of the output current of inverter $\boldsymbol{i}_{\text{i}}$ is as follows:

$$\begin{aligned}\boldsymbol{i}_{i} &= \boldsymbol{I}_{\text{res}} + \boldsymbol{I}_{lk} + \boldsymbol{I}_{\text{G}\sum}\\ &= \boldsymbol{I}_{\text{res}} + \left(\frac{3Z_{F} + Z_{F}G_{\Sigma}Z_{\sum lk}^{-1}}{3Z_{F}Z_{\sum lk} + Z_{\sum lk}G_{\Sigma} + Z_{F}G_{\Sigma}} - 1\right)\boldsymbol{U}_{N\_res}.\end{aligned} \tag{13}$$

It should be noticed that expression of $\boldsymbol{i}_{\text{i}}$ for compensating the residual fault current to zero can be obtained via setting $\boldsymbol{I}_{\text{res}}$ to zero. The current $\boldsymbol{I}_{\text{full\_com}}$ for full ground-current compensation is defined as the current injected to neutral, which ensures the ground current to be zero under the conditions of ground impedance variation.

$$\begin{aligned}\boldsymbol{I}_{\text{full\_com}} &= \left(\frac{3Z_{F} + Z_{F}G_{\Sigma}Z_{\sum lk}^{-1}}{3Z_{F}Z_{\sum lk} + Z_{\sum lk}G_{\Sigma} + Z_{F}G_{\Sigma}} - 1\right)\boldsymbol{U}_{N\_res}\\ &= \left(3 - \frac{9Z_{F}Z_{\sum lk}G_{\Sigma}^{-1} + 3Z_{F}}{3Z_{F}Z_{\sum lk} + Z_{\sum lk}G_{\Sigma} + Z_{F}G_{\Sigma}}\right)\boldsymbol{U}_{C}.\end{aligned} \tag{14}$$

Obviously, if the injected current $\boldsymbol{i}_{\text{i}}$ is controlled to be equivalent to $\boldsymbol{I}_{\text{full\_com}}$, the faulty phase voltage and ground-fault residual current will be limited to zero, and thus the fault arc can be extinguished. The neutral-to-ground voltage can be adjusted to expectation value, then, the neutral voltage error can be erased.

Therefore, it is necessary to analysis the relationship between $\boldsymbol{i}_{\text{i}}$ and $\boldsymbol{U}_{\text{i}}$, since the active ASD is treated as voltage source in our case. According to Thevenin–Norton theorem, the active ASD equivalent impedance Z_{i} is in parallel with ground-fault resistance and the impedance of the distribution network as well as the leakage impedances of transformers, expressed as follows:

$$Z_{i} = \frac{Z_{F}G_{\Sigma}Z_{\sum lk}}{Z_{F}G_{\Sigma} + (3Z_{F} + G_{\Sigma})Z_{\sum lk}}. \tag{15}$$

Then, following the Ohm's law, the active ASD voltage $\boldsymbol{U}_{\text{i}}$ can be obtained as follows:

$$\boldsymbol{U}_{i} = Z_{i}\boldsymbol{i}_{i} = \frac{Z_{F}G_{\Sigma}Z_{\sum lk}}{Z_{F}G_{\Sigma} + (3Z_{F} + G_{\Sigma})Z_{\sum lk}}\boldsymbol{i}_{i}. \tag{16}$$

The active ASD voltage $\boldsymbol{U}_{\text{i}}$ is controlled to reach the expectation value as (16) so that the output current $\boldsymbol{i}_{\text{i}}$ can be equal to $-\boldsymbol{i}_{\text{sum}}$, which compensates the neutral voltage error and restrain residual fault current at the same time. The compared amplitudes of active power between passive ASD and active ASD are shown as bellow, where the passive ASD equivalent impedance is Z_{F}//

TABLE II
PARAMETERS OF THE SIMULATED DISTRIBUTION NETWORK

Parameter	VALUE	PER-UNIT
Turn ratio of $T_1(N_{p1}/N_{p1}/N_{s1})$	10/10/0.4	-
Turn ratio of T_2 (N_{p2}/N_{s2})	10/0.4	-
Nominal ground-fault current	100A	-
Nominal value of distribution line	10kV	-
Power capacity of T_1	500kVA	-
Power capacity of T_2	500kVA	-
Base capacity	1000kVA	-
Base voltage	10kV	-
Line-to-ground resistance R_S	10kΩ	100
Line-to-ground capacitance C_S	8.36μF	3.81
Leakage inductance of T_1 $(Z_{lk\text{-}T1})$	18.39μH	5.8e-5
Leakage inductance of T_2 $(Z_{lk\text{-}T2})$	0.405μH	1.3e-6
Frequency ω_0	50 Hz	-
Grounding fault resistance Z_F	10Ω, 10kΩ	0.1, 100

$G_\Sigma + Z_{\Sigma lk}$.

$$P_{active} = \mathrm{Re}\left(\boldsymbol{i}_i^2 \frac{Z_F G_\Sigma Z_{\sum lk}}{Z_F G_\Sigma + (3Z_F + G_\Sigma) Z_{\sum lk}}\right) \tag{17}$$

$$P_{passive} = \mathrm{Re}\left(\boldsymbol{U}_N^2 \frac{3Z_F + G_\Sigma}{Z_F G_\Sigma + (3Z_F + G_\Sigma) Z_{\sum lk}}\right). \tag{18}$$

Take notice that the zero-sequence impedance of the transformers has a magnitude $Z_{\Sigma lk} = N_{T2}{}^2 Z_{lk\text{-}T1} + Z_{lk\text{-}T2}$ of less than 1 from Table II, the magnitude of $\boldsymbol{i}_i$ is smaller than that of $\boldsymbol{U}_N$, and they both share the same denominator in (17) and (18). Therefore, the active power of active ASD P_{active} is way less than that of passive ASD $P_{passive}$. According to values in Table II and (17) and (18), the capacity of active part is 12.4% of total in the proposed method.

2) Asymmetric Distribution Network: Principle of passive ASD method is the same in either symmetric or asymmetric system. Assume passive ASD has been activated as SLG fault on phase C, resulting on ground-fault current $\boldsymbol{I}_F$ being constraint down to the residual current $\boldsymbol{I}_{res}$. The algorithm of active ASD method in asymmetric distribution network is presented below, where all the parameters are shown in Table I. In asymmetric distribution network, the neutral-to-ground voltage becomes unbalanced. Hence, $\boldsymbol{U}_{00}$ denotes neutral unbalanced voltage, after the operation of passive part in hybrid ASD, we assume $\boldsymbol{U}_{00} = -\boldsymbol{U}_C$. Parameter relationships among three phases can be simplified by using the rotating coefficient $a = e^{j2\Pi/3}$. Thus, analysis of the principle of Nodal-Voltage method in Fig. 3 without the active ASD part is presented in (19) and (20), the voltage between dot "$_1$" and "$_0$", $\boldsymbol{U}_{10}$ can be obtained, where $Y_{\Sigma 10}$ denotes equivalent admittance between dot "$_1$" and "$_0$".

$$\begin{aligned} \boldsymbol{U}_{10} = &-Y_{\sum 10}{}^{-1}[\alpha^2 Z_A{}^{-1} + \alpha Z_B{}^{-1} \\ &+ (Z_C//Z_F)^{-1} + Z_{\sum lk}{}^{-1}]\boldsymbol{U}_C \end{aligned} \tag{19}$$

$$Y_{\sum 10} = Z_A{}^{-1} + Z_B{}^{-1} + (Z_C//Z_F)^{-1} + Z_{\sum lk}{}^{-1}. \tag{20}$$

According to Kirchhoff's theorem, the new expression of the output current of inverter $\boldsymbol{i}_{i\text{-asy}}$ in Fig. 3 can be calculated as follows:

$$\boldsymbol{i}_{i-asy} = \boldsymbol{I}_A + \boldsymbol{I}_B + \boldsymbol{I}_C + \boldsymbol{I}_F + (\boldsymbol{U}_{10} - \boldsymbol{U}_{00}) Z_{\sum lk}{}^{-1} \tag{21}$$

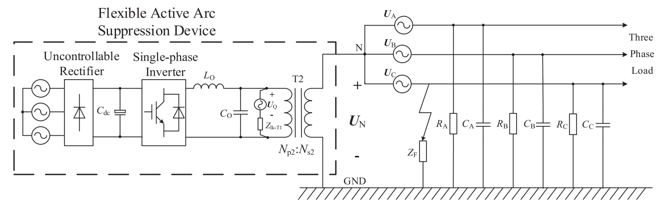

Fig. 6. Simplified distribution network.

$$\text{where} \begin{cases} I_A = (\boldsymbol{U}_{10} + \boldsymbol{U}_A) Z_C{}^{-1} \\ I_B = (\boldsymbol{U}_{10} + \boldsymbol{U}_B) Z_B{}^{-1} \\ I_C = (\boldsymbol{U}_{10} + \boldsymbol{U}_C) Z_C{}^{-1} \\ I_F = (\boldsymbol{U}_{10} + \boldsymbol{U}_C) Z_F{}^{-1} \end{cases}.$$

That is, via setting $\boldsymbol{I}_F$ to zero and the output current of inverter $\boldsymbol{i}_i$ can be set as to be the opposite of summed current $\boldsymbol{i}_{sum\text{-}asy}$, then complete arc suppression can be achieved.

Basically, the advantage by using hybrid ASD method is that it costs less for sustaining little active device capacity. Passive ASD method is applied for high-power compensation in ground-fault current, then, the inverter-input (active ASD) voltage is controlled to generate the current for the compensation to the neutral voltage error, which allows the neutral-to-ground voltage to be controlled as expectation value.

III. ACTIVE ARC-SUPPRESSION METHOD

A. Model of Distribution Network

Typical parameters for case study are presented in Table II. The distribution network is a 10 kV power system shown in Fig. 6. As the bolted ground fault rarely happens, the ground-fault resistance Z_F is chosen to be 10 to 10 kΩ in case study [20]. Thus, the power stage of the distribution network is in fundamental frequency, in which the distribution network can be treated as series connected voltage source $\boldsymbol{E}_0$ and zero-sequence impedance of the distribution network Z_0, expressed in (22) and (23), where R_S, C_S are set as the symmetric line-to-ground parameters of three-phase

$$\boldsymbol{E}_0 = \frac{\boldsymbol{U}_C}{N_{T2}} \frac{R_S}{3sZ_F R_S C_S + 3Z_F + R_S} \tag{22}$$

$$Z_0 = \frac{Z_F R_S}{(3sZ_F R_S C_S + 3Z_F + R_S) N_{T2}^2}. \tag{23}$$

We assume SLG fault happens on phase C. The equivalent voltage source in (22) is the symmetric voltage caused by the line-to-ground parameters while the equivalent impedance Z_0 in (23) stands for the load of the proposed ASD. Take notice that the leakage impedance $Z_{lk\text{-}T2}$ of single-phase isolation transformer T_2 is neglected as it is relatively small (less than 7% of the output inductance) in our case.

Since the converted voltage and impedance is in parallel with the line-to-ground voltage $\boldsymbol{u}_Q$ series connected with the leakage impedance $Z_{lk\text{-}T1}$ of zig-zag grounding transformer T_1. Assume the two transformers are completely under control, and then the distribution network model can be converted to the low-voltage side of the single-phase isolation transformer T_2. According to

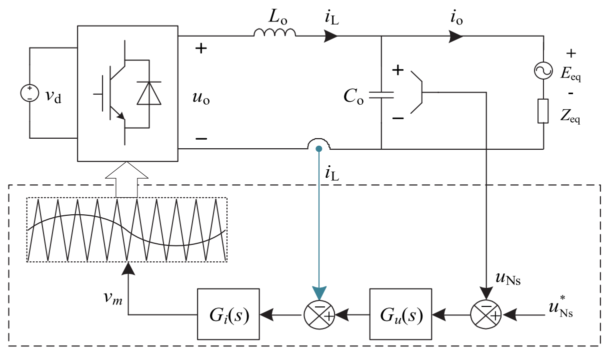

Fig. 7. Equivalent circuit of distribution network.

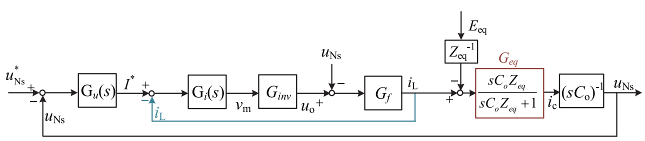

Fig. 8. Simplified block diagram of the dual-loop control diagram.

Thevenin theorem, we can obtain an equivalent voltage $\boldsymbol{E}_{\mathrm{eq}}$ and an equivalent impedance Z_{eq} from the distribution network with the influence of leakage impedance from T_1.

$$\boldsymbol{E}_{\mathrm{eq}} = \left(\frac{\boldsymbol{u}_{\mathrm{Q}}}{Z_{lk-T1}} + \frac{\boldsymbol{U}_{\mathrm{C}}N_{T2}}{Z_F}\right) Z_{eq} \tag{24}$$

$$Z_{\mathrm{eq}} = Z_{\mathrm{lk}-T1}//Z_0. \tag{25}$$

B. Voltage Control Method

In order to guarantee that the neutral-to-ground voltage ($\boldsymbol{U}_{\mathrm{N}}$) can track the inverse of the line-to-neutral voltage of faulty phase, a typical dual-loop control method is employed in the proposed hybrid ASD. No need to measure the zero-sequence admittance, capacitor current and so forth, the feedback controls the amplitude and phase of the injected current, forcing the voltage of the fault phase to zero, compensating the phase error of neutral voltage by adjusting the neutral voltage to the expectation value, which can erase the neutral voltage error. Then, the hybrid ASD method reaches to the purpose of voltage arc suppression.

The method includes a neutral-to-ground voltage outer loop and an output inductor current inner loop and the control algorithm determines the dynamic performance of the single-phase inverter. The error of U_{N} is then regulated by a PR regulator to generate the reference of the injected current I^*, which is the control objective of the inner-control loop. Thus, the filter inductor current feedback (ICF) is adopted in the inner loop for enhancing the system tolerance ability to load disturbances, as shown in Fig. 7, where $U_{Ns}{}^*$ is the opposite voltage of faulty phase supply voltage, u_{o} is output voltage from single-phase inverter.

The voltage control diagram in Fig. 7 can be further simplified as Fig. 8, where the simplified transfer function of filter $G_f(s)$ is $(sL_o + r)^{-1}$, G_{inv} is inverter gain K_{inv} and the transfer function of PR controller G_i (s) is shown in (26), where ζ denotes damping

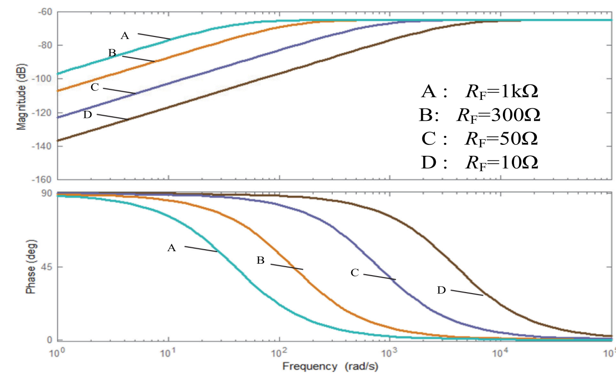

Fig. 9. Bode diagram of G_{eq} when RF varies and CS is nominal. (Frequency: rad/s).

coefficient, ω_0 is fundamental frequency, K_{cp} is proportionality coefficient, and K_{cr} is resonant coefficient.

$$G_i(s) = K_{cp} + \frac{K_{cr}s}{s^2 + 2\zeta\omega_0 s + \omega_0^2}. \tag{26}$$

From Fig. 8, the transfer function of the voltage control system can be attained. The stability error of $\boldsymbol{U}_{\mathrm{Ns}}$ (considered low frequency) near the power frequency is very subtle because of the PR controller. Hence, the transfer function of both current-open loop H_{i} and inner loop G_{inner} are expressed as follows:

$$\begin{aligned} H_i(s) &= G_i(s) \cdot G_{inv}(s) \cdot G_f(s) \\ &= \left(K_{cp} + \frac{K_{cr}s}{s^2 + 2\zeta\omega_0 s + \omega_0^2}\right) \cdot K_{inv} \cdot \frac{1}{sL_0 + r}. \end{aligned} \tag{27}$$

The additional function G_{eq} to the forward path comparing to the ICF method is marked in Fig. 8.

$$\begin{aligned} &G_{eq} \\ &= \frac{sC_oR_SZ_{lk-T1}}{sC_oR_SZ_{lk-T1}+(3sR_SC_S+3+Z_F^{-1}R_S)N_{T2}^2Z_{lk-T1}+R_S}. \end{aligned} \tag{28}$$

Apparently, G_{eq} is a first-order high pass filter with a small gain, which depends on the ground-fault resistance and distributed capacitance. Fig. 9 shows the Bode diagram of G_{eq} when R_{F} increases, demonstrating that the fundamental gain in low-resistance grounding is lower than the one in high-resistance. Fig. 10 presents the Bode diagram of as C_{S} varies. When C_{S} increases, the high-band gain decreases, which indicates that the light load has lower antiinterference ability than heavy load. Both Figs. 9 and 10 can prove the great stability of the dual-loop control under different conditions.

Furthermore, the outer voltage loop of the controller is designed to achieve zero steady-state error in fundamental frequency and enough damping to compensate the ground-fault phase error of neutral voltage. In order to avoid the calculation burden of the processor, simply PI plus resonant controller is

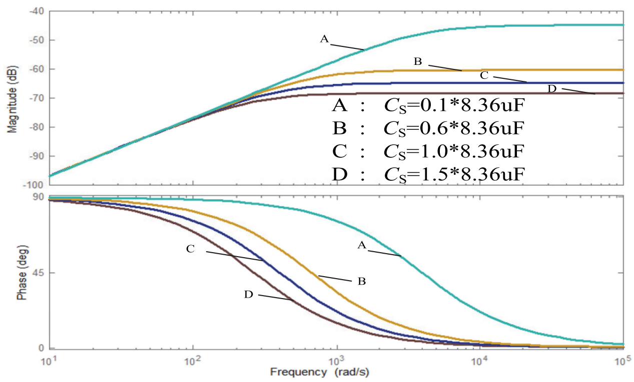

Fig. 10. Bode diagram of G_{eq} as CS varies and RF = 100 Ω. (Frequency: rad/s).

applied to achieve good control performance [20].

$$G_u(s) = K_p + \frac{K_i}{s} + \frac{2K_r s}{s^2 + \omega_0^2}. \tag{29}$$

Therefore, the transfer function of U_{Ns} can be obtained from Fig. 8, where we can find the transfer function of the entire controller expressed as follows:

$$U_{Ns} = G_1 U_{Ns}^* + G_2 E_{eq}. \tag{30}$$

Where

$$G_1 = \frac{G_u G_{\mathrm{inner}}}{sC_0 + G_f + (Z_{\mathrm{eq}})^{-1} + G_u G_{\mathrm{inner}}}$$
$$G_2 = \frac{G_{\mathrm{inner}} - 1}{Z_{\mathrm{eq}} G_f G_{\mathrm{inner}} + (sC_0 Z_{\mathrm{eq}} + 1)(1 - G_{\mathrm{inner}})}.$$

The control parameters are tuned by using the frequency domain design method. The current loop has a cutoff frequency of 1/10 of the switching frequency f_{sw} and the voltage loop has a cutoff frequency of 1/2 of the current loop cutoff frequency. Their phase margins are both set to 45°. These values can be used to calculate the control parameters and slight change of the parameters is necessary due to the mismatch of the theoretical and practical model.

C. Implementation

For potential practical application, it should be noted that the hybrid ASD mainly focuses on the full compensation of grounding fault current, while the recognition of faulty state is fully and precisely accomplished before the hybrid ASD takes actions [21].

The implementation flowchart of the proposed hybrid ASD is given in Fig. 11. First, when the neutral point displacement voltage exceeds 15% of nominal phase voltage, an SLG fault is confirmed and the faulty phase is identified [21]. Second, the corresponding multiterminal breakers (refers to Table I) are closed for primarily regulating the zero-sequence voltage $\boldsymbol{U}_{\mathrm{N}}$. Finally, to fully compensate the voltage regulation error brought by leakage inductances of T_1 and T_2, the active ASD then inputs current $\boldsymbol{i}_{\mathrm{i}}$ to the neutral point by the voltage control method

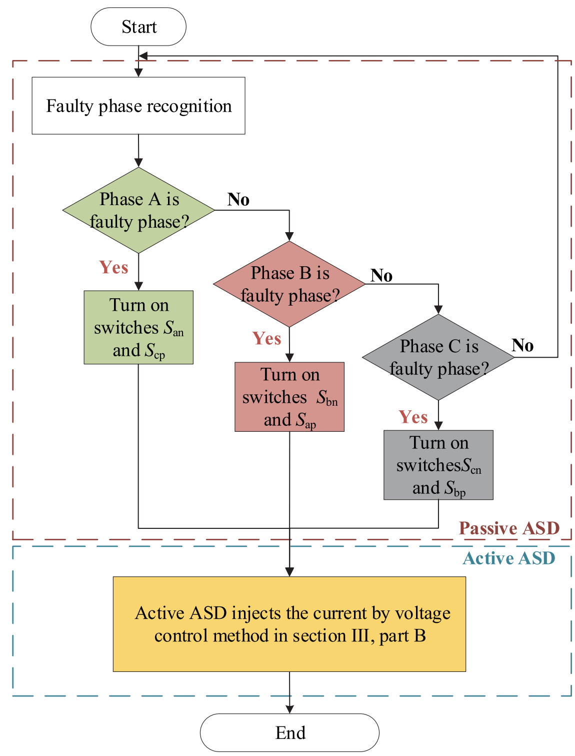

Fig. 11. Implementation flowchart of the proposed hybrid ASD device.

TABLE III
PARAMETERS OF DESIGNED CONTROLLER

Parameter	VALUE
Switch frequency f_{sw}	10kHz
Filter inductance L_o	0.5 mH
Filter inductor ESR r	0.2Ω
Filter capacitance C_o	10μF
Inverter gain K_{inv}	259.8
Inner-loop proportional ratio K_{cp}	45
Inner-loop Resonant ratio K_{cr}	100
The damping coefficient ζ	0.05
Outer-loop proportional ratio K_p	4.1
Outer-loop integral ratio K_i	73.4
Outer-loop Resonant ratio K_r	1

in Section III, part B. Therefore, the system can achieve the accurate arc suppression after the SLG fault.

IV. SIMULATION VERIFICATION

In order to validate the performance of the proposed hybrid ASD, the distribution network and the hybrid ASD as shown in Fig. 1 are modeled and simulated in MATLAB/Simulink. The method introduced in Section III.C is used to design the controller. The parameters of the distribution network are listed controller. The parameters of the distribution network are listed in Table II, and the controller parameters are listed in Table III.

In the simulations, an SLG fault is applied to phase A of the distribution network at 0.4 s. To better compare the control effect of the passive ASD and the hybrid ASD, the passive ASD is activated at 0.5 s with the active ASD deactivated, while the active ASD is activated at 0.6 s with the passive ASD activated

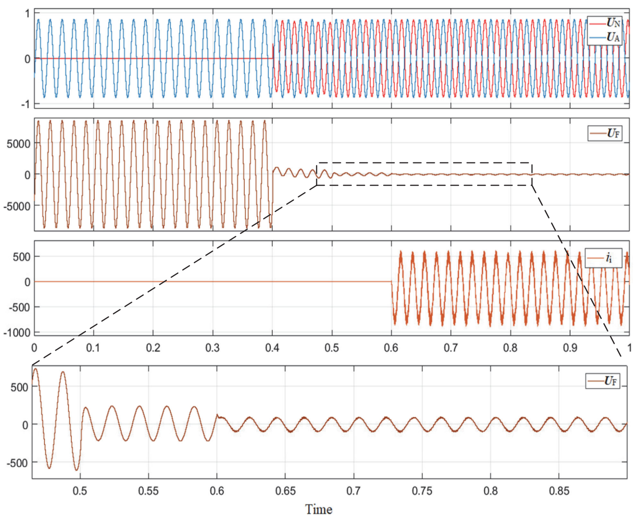

Fig. 12. Simulation result under a SLG fault on phase A (ZF = 10 Ω).

TABLE IV
COMPARISON OF FAULTY PHASE VOLTAGE AND CURRENT

Ground-fault resistance	Passive ASD only		Hybrid ASD (Passive + Active)		Bidirectional Power flow
Z_F/Ω	I_F/A	U_F/V	I_F/A	U_F/V	
10	22.6	234.5	4.4	46.8	NO
10k	0.046	452.6	0.0095	96.4	NO
10	23.4	230.2	10.4	105	YES
10k	0.0392	399.1	0.016	157.2	YES

as well. Two different fault resisters are simulated, 10 Ω and 10 kΩ.

Fig. 12 shows the waveforms of the neutral-to-ground voltage ($\boldsymbol{U}_{\rm N}$), phase A positive sequence voltage ($\boldsymbol{U}_{\rm A}$), the fault phase voltage ($\boldsymbol{U}_{\rm F}$), and the injected current from the inverter ($\boldsymbol{i}_{\rm i}$), when the fault resistance is 10 Ω. Started from 0.4 s, the single-phase isolation transformer ($\rm T_2$) is accessed after closing S_{an} and S_{cp} (fault on phase A) in the multiterminal breakers to regulate the line-to-line voltage $\boldsymbol{u}_{\rm Q}$. At 0.5 s, the passive ASD is activated without the controlled current $\boldsymbol{i}_{\rm i}$ from the active ASD. The magnitude of the fault phase voltage ($\boldsymbol{U}_{\rm F}$) is reduced from 658.2 V to less than 234.5 V. After the active ASD is activated at 0.6 s, the faulty phase voltage ($\boldsymbol{U}_{\rm F}$) can be further reduced to 46.8 V, because of the full compensation of the phase error of the neutral voltage. Meanwhile, the neutral-to-ground voltage $\boldsymbol{U}_{\rm N}$ can equal to the opposite of the fault-phase supply voltage $\boldsymbol{U}_{\rm A}$.

Similarly, when the same fault occurs on phase A with 10 kΩ fault resistance, the simulation results are given in Fig. 13. With the passive ASD activated only, the fault phase voltage ($\boldsymbol{U}_{\rm F}$) can decrease from 8500 to 452.2 V at 0.5 s. It can be further reduced to 96.4 V after active ASD activated at 0.6 s.

Moreover, the proposed hybrid ASD is tested under bidirectional power flow conditions. The results are summarized in Table IV. It is demonstrated that the residue fault current and fault phase voltage can further decrease after the active ASD is activated.

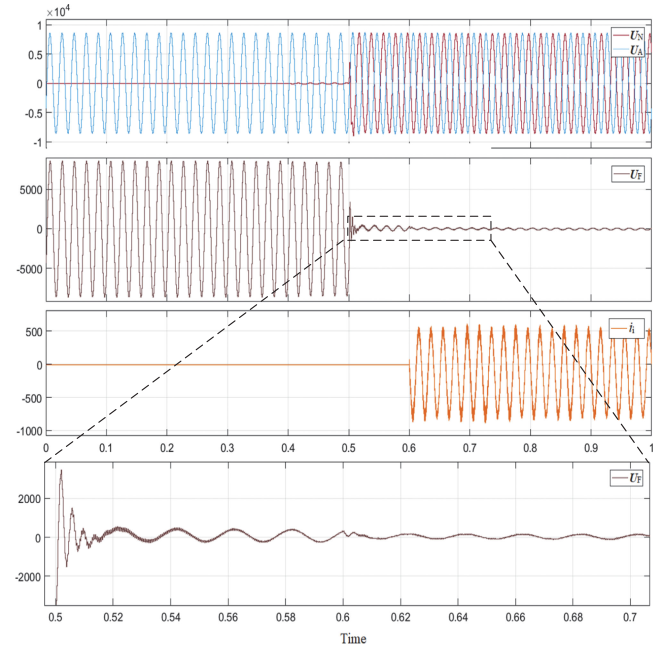

Fig. 13. Simulation result under a SLG fault on phase A (ZF = 10 kΩ).

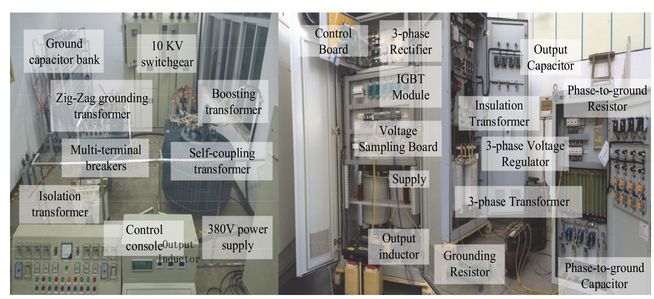

Fig. 14. Experimental platform for flexible grounding system of distribution network.

V. EXPERIMENT VERIFICATION

To further validate the performance of the proposed hybrid ASD in a more realistic condition, a hybrid ASD prototype has been developed and tested in an emulated distribution network.

As shown in Fig. 14, 10 kV power supply system is formed by a 380 V power supply, a self-coupling transformer and a boosting transformer. The main circuit of the active device consists of a three-phase control rectifier and a single-phase full-bridge inverter with an LC type filter. The rated voltage and current of the IGBT modules of the inverter are 1200 V and 400 A, respectively. The digital signal controller TMS320F28335 from Texas Instruments is used as the controller of power electronic switches. The other parts of the experimental system are the same as in Fig. 1. The parameters of the distribution network and the hybrid ASD are the same as the simulation in MATLAB/Simulink in Section IV. The test scenarios in Section IV are duplicated in this experiment for comparison.

Fig. 15 gives the neutral-to-ground voltage ($\boldsymbol{U}_{\rm N}$), phase A positive sequence voltage ($\boldsymbol{U}_{\rm A}$), the fault phase voltage ($\boldsymbol{U}_{\rm F}$),

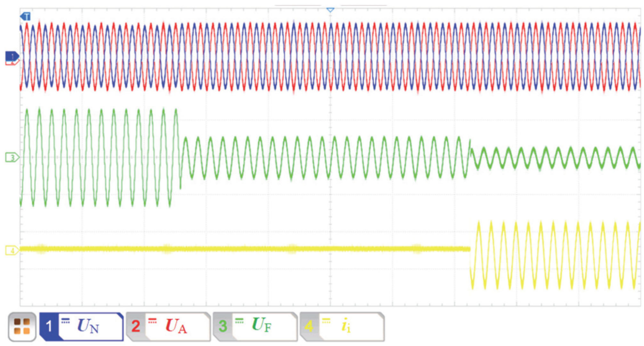

Fig. 15. Experiment result under a SLG fault on phase A (ZF = 10 Ω). CH1: Neutral-to-ground voltage (6000 V/div, t:0.1s/div). CH2: Positive-sequence voltage (6000 V/div, t:0.1s/div)CH3: Ground-fault voltage (280V/div, t:0.1s/div)CH4: Active ASD injected current (250A/div, t:0.1s/div).

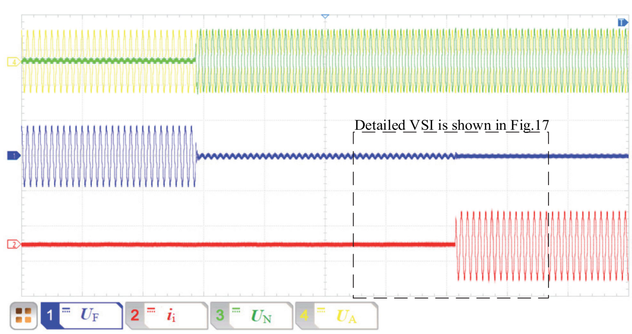

Fig. 16. Experiment result under a SLG fault on phase A (ZF = 10 kΩ). CH1: Neutral-to-ground voltage (6000 V/div, t:0.1s/div). CH2: Positive-sequence voltage (6000 V/div, t:0.1s/div)CH3: Ground-fault voltage (280V/div, t:0.1s/div)CH4: Active ASD injected current (250A/div, t:0.1s/div)

and the injected current from the inverter ($\boldsymbol{i}_{\mathrm{i}}$), when the fault resistance is 10 Ω. Again, the passive ASD is first activated after the SLG fault occurs. About 0.5 s later, the active ASD is activated. As shown in Fig. 15, the fault phase voltage is reduced to 221 V when only passive ASD is activated, and further reduced to 58.5 V after the active ASD is activated. Meanwhile, the faulty residual current is reduced to 5.74 A with the hybrid ASD, and the faulty current rejection ratio is 0.97%.

When the fault resistance is 10 kΩ, since the voltage measurements are out of the range of the existing oscilloscope, additional sensors are added to capture the accurate experiment results. The experiment results are given in Figs. 16 and 17.

The faulty phase voltage and current are reduced to 123 V and 0.013 A, respectively, after the hybrid ASD is applied. The faulty current rejection ratio is 2.07%. In Fig. 16, fast dynamic response can be observed from the faulty phase voltage. According to the theoretical analysis, the voltage error after the change of capacitance is treated as the open-loop bandwidth decrease. Therefore, it is demonstrated that the proposed hybrid ASD can handle SLG faults with different ground-fault resistances.

The trajectory of phase error of neutral voltage compensation is given in Fig. 18, where four different ground-fault resistances

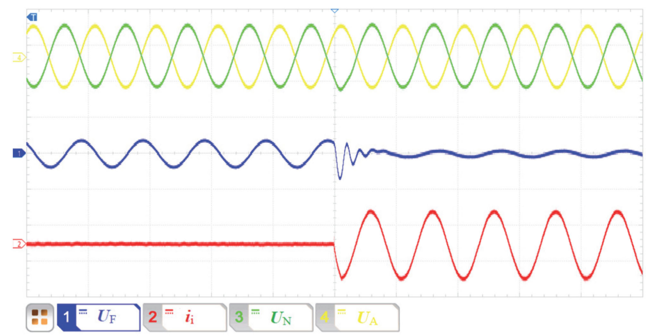

Fig. 17. Detailed experiment result under a SLG fault on phase A (Z_F = 10 kΩ). CH1: Ground-fault voltage (750V/div)CH2: Active ASD injected current (250A/div, t:0.02s/div)CH3: Zero-sequence voltage (6000 V/div, t:0.02s/div)CH4: Positive-sequence voltage (6000 V/div, t:0.02s/div).

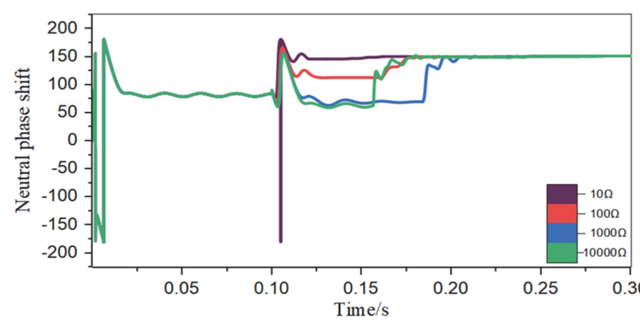

Fig. 18. Compensation trajectory in phase error of neutral voltage by ASD when 10, 100, 1000, and 7000 Ω fault in distribution network.

(10 Ω, 100 Ω, 1 kΩ, and 10 kΩ) are compared. The SLG fault occurs at 0.1 s, and the faulty phase can be all successfully recognized within 0.06 s. During 0.16 to 0.23 s, the ASD without the assistance of single-phase VSI is activated for confirming the fault arc cannot be rekindled. After 0.23 s, the phase error is fully compensated for complete-elimination in ground-fault arc, simply by injecting the current from the VSI within few microseconds. The phase error of neutral voltage in multiple ground-fault resistances is compensated by the hybrid ASD. Eventually, all the trajectories overlap to each other, which demonstrate the feasibility of the hybrid ASD.

Note that the advantage of the ASD is presented with the compared performances in two groups and a detailed trajectory of compensation in phase error of neutral voltage in different resistance grounding faults.

Most of conventional methods are equipped with isolation transformers; the advantage of the proposed method is that it only needs to add six breakers to the conventional methods with small capacity electronic devices to achieve flexible arc suppression with full compensation of fault current. For the purpose of demonstrating great performance in hybrid ASD, conventional methods under same conditions are recorded in Table V with major performance parameters, where T_{dev} is the total time of the process and C_{ap} is capacity of the needed electronic device in ASD. Note that hybrid ASD has the fastest

TABLE V
COMPARATIVE EXPERIMENT RESULTS IN FUNDAMENTAL DOMAIN

Types	U_F/V	I_F/A	T_{dev}/s	C_{ap}/kVA	Z_F
ASC	102	10.5	0.15	0	10Ω
	231	0.0226	0.24	0	10kΩ
Voltage-based ASD	76	7.54	0.02	20	10Ω
	182.1	0.0179	0.03	20	10kΩ
Hybrid ASD	58.5	5.74	0.09	0.78	10Ω
	123	0.013	0.07	0.78	10kΩ

TABLE VI
COMPARATIVE CHARACTERISTICS IN DIFFERENT ARC-SUPPRESSION METHODS

Types	*Detection complexity*	*Reliability*	*Control complexity*	*Cost*	*Arc suppression effectiveness*
Peterson coil	HIGH	HIGH	LOW	MEDIUM	LOW
Voltage-based ASD	LOW	LOW	HIGH	HIGH	HIGH
Fault-transfer Switch	HIGH	LOW	LOW	HIGH	HIGH
Proposed Hybrid ASD	LOW	MEDIUM	MEDIUM	MEDIUM	HIGH

response ($T_{\mathrm{dev}} \leq 0.03$ s) as SLG fault occurs in the distribution network, while the performance of hybrid ASD surpass the other two conventional methods, with total capacity of electronic equipment is far less than voltage-based inverter ASD. Great advantages in hybrid ASD have inhibited in Table VI.

Different characteristics are listed in Table VI for comparison of different arc-suppression methods. Peterson coil has high reliability and low-control complexity, but it needs to detect the capacitive current, which is difficult to be guaranteed. Voltage-based ASD does not need to detect the capacitive current and has better arc suppression effect. However, large capacity power electronics devices suffer from low reliability and high cost. Fault-transfer switch, as a passive method, also has high reliability, however, it may cause line-to-line fault if the faulty phase is falsely identified.

As the proposed hybrid ASD is a voltage arc suppression method, it does not need to detect the capacitive current. The ground-fault current compensation is primarily done by the passive ASD, and the residual current is easily eliminated by the small capacity active ASD. Thus, the proposed hybrid ASD brings better arc suppression effect, relatively high reliability, low cost, and control complexity.

VI. CONCLUSION

This article presented a hybrid ground-fault arc suppression device, which took great advantage of the reliability of passive device and the flexibility of active device. Zero-sequence voltage regulation was primarily done by reliable passive device, and precise compensation of ground-fault residual current was realized by the active device, which obtained full compensation of SLG fault current.

Peterson coils, voltage-based ASD, fault-transfer switch and the proposed hybrid ASD were comparatively analyzed in detection complexity, reliability, control complexity, and cost and arc suppression effectiveness. It illustrated that the proposed device had comprehensive advantages of high reliability, low-cost, and low-control complexity, which could achieved full compensation of ground-fault current.

REFERENCES

[1] X. Wang *et al.*, “Location of single phase to ground faults in distribution networks based on synchronous transients energy analysis,” *IEEE Trans. Smart Grid*, vol. 11, no. 1, pp. 774–785, Jan. 2020.

[2] W. Qiu, M. Guo, G. Yang, and Z. Zheng, “Model-predictive-control-based flexible arc-suppression method for earth fault in distribution networks,” *IEEE Access*, vol. 7, pp. 16051–16065, 2019.

[3] P. Wang, B. Chen, C. Tian, B. Sun, M. Zhou, and J. Yuan, “A novel neutral electromagnetic hybrid flexible grounding method in distribution networks,” *IEEE Trans. Power Del.*, vol. 32, no. 3, pp. 1350–1358, Jun. 2017.

[4] *IEEE Recommended Practice for Grounding of Industrial and Commercial Power Systems*, IEEE Std 142-2007 (Revision of IEEE Std. 142-1991), Nov 2007.

[5] P. S. Moses, M. A. S. Masoum, and H. A. Toliyat, “Impacts of hysteresis and magnetic couplings on the stability domain of ferroresonance in asymmetric three-phase three-leg transformers,” *IEEE Trans. Energy Convers.*, vol. 26, no. 2, pp. 581–592, Jun. 2011.

[6] X. Zeng, Y. Xu, and Y. Wang, “Some novel techniques for insulation parameters measurement and petersen-coil control in distribution systems,” *IEEE Trans. Ind. Electron.*, vol. 57, no. 4, pp. 1445–1451, Apr. 2010.

[7] A. Cerretti, F. M. Gatta, A. Geri, S. Lauria, M. Maccioni, and G. Valtorta, “Ground fault temporary overvoltages in MV networks: Evaluation and experimental tests,” *IEEE Trans. Power Del.*, vol. 27, no. 3, pp. 1592–1600, Jul. 2012.

[8] R. Burgess and A. Ahfock, “Minimising the risk of cross-country faults in systems using arc suppression coils,” *IET Gener., Transmiss. Distrib.*, vol. 5, no. 7, pp. 703–711, Jul. 2011.

[9] S. K. Dash *et al.*, “Realization of active power filter based on indirect current control algorithm using xilinx system generator for harmonic elimination,” *Int. J. Elect. Power Energy Syst.*, vol. 74, pp. 420–428, 2016.

[10] W. Wang, L. Yan, X. Zeng, B. Fan, and J. M. Guerrero, “Principle and design of a single-phase inverter-based grounding system for neutral-to-ground voltage compensation in distribution networks,” *IEEE Trans. Ind. Electron.*, vol. 64, no. 2, pp. 1204–1213, Feb. 2017.

[11] W. Wang, L. Yan, B. Fan, and X. Zeng, “Control method of an arc suppression device based on single-phase inverter,” in *Proc. Int. Symp. Power Electron., Elect. Drives, Autom Motion*, 2016, pp. 929–934.

[12] X. Li *et al.*, “A generalized design framework for neutral point voltage balance of three-phase vienna rectifiers,” *IEEE Trans. Power Electron.*, vol. 34, no. 10, pp. 10221–10232, Oct. 2019.

[13] A. Gargoom *et al.*, “Residual current compensator based on voltage source converter for compensated distribution networks,” in *Proc. IEEE Power Energy Soc. Gen. Meeting*, 2018, pp. 1–5.

[14] A. D. Conti *et al.*, “Effect of a lossy dispersive ground on lightning overvoltages transferred to the low-voltage side of a single-phase distribution transformer,” *Electric Power Syst. Res.*, vol. 153, pp. 104–110, 2017.

[15] Z. Xu, B. Li, S. Wang, S. Zhang, and D. Xu, “Generalized single-phase harmonic state space modeling of the modular multilevel converter with zero-sequence voltage compensation,” *IEEE Trans. Ind. Electron.*, vol. 66, no. 8, pp. 6416–6426, Aug. 2019.

[16] H. Nouri and M. M. Alamuti, “Comprehensive distribution network fault location using the distributed parameter mo del,” *IEEE Trans. Power Del.*, vol. 26, no. 4, pp. 2154–2162, Oct. 2011.

[17] P. Toman, M. Paar, and J. Orsagova, “Possible solutions to problems of voltage asymmetry and localization of failures in MV compensated networks,” in *Proc. IEEE Lausanne Power Tech.*, 2007, pp. 1758–1763.

[18] *IEEE Guide for the Application of Tertiary and Stabilizing Windings in Power Transformers*, IEEE Std C57.158-2017, Apr. 2018.

[19] J. Meng *et al.*, “Zero-sequence voltage trajectory analysis for unbalanced distribution networks on single-line-to-ground fault condition,” *Electric Power Syst. Res.*, vol. 161, pp. 17–25, 2018.

[20] W. Wang, X. Zeng, L. Yan, X. Xu, and J. M. Guerrero, “Principle and control design of active ground-fault arc suppression device for full compensation of ground current,” *IEEE Trans. Ind. Electron.*, vol. 64, no. 6, pp. 4561–4570, Jun. 2017.

[21] B. Fan *et al.*, “Faulty phase recognition method based on phase-to-ground voltages variation for neutral ungrounded distribution networks,” *Electric Power Syst. Res.*, vol. 190, 2021, Art. no. 106848.

Bishuang Fan (Member, IEEE) received the M.S. degree in automation of electric power system from the Changsha University of Science and Technology, Changsha, China, in 2007 and the Ph.D. degree in control science and engineering from Central South University, 2014.

He is an Associate Professor with the School of Electrical and Information Engineering, Changsha University of Science and Technology. His current research interests include power conversion technologies.

Ganzhou Yao (Student Member, IEEE) was born in Guangdong Province, China, in 1995. He received the B.S. degree in electrical engineering and automation, in 2014 from Chengnan College, Changsha University of Science and Technology, Changsha, China, where he is currently working toward the M.S. degree in electrical engineering.

His research interests include power electronic technology in grounding systems.

Wen Wang (Member, IEEE) received the B.S. and Ph.D. degrees in electrical engineering from Hunan University, Changsha, China, in 2008 and 2013, respectively.

He is an Associate Professor with the School of Electrical and Information Engineering, Changsha University of Science and Technology. His current research interests focus on flexible grounding methods in distribution networks.

Xiangjun Zeng (Senior Member, IEEE) received the M.S. degree in 1996 from Wuhan University, Wuhan, China, and the Ph.D. degree from the Huazhong University of Science and Technology, in 2001, both in electrical engineering.

He is a Full Professor with the School of Electrical and Information Engineering, Changsha University of Science and Technology. His research interests include real-time computer application in power systems protection and control.

Josep M. Guerrero (Fellow, IEEE) received the Ph.D. degree in power electronics from the Technical University of Catalonia, Barcelona, Spain, in 2003.

Since 2011, he has been a Full Professor with the Department of Energy Technology, Aalborg University, Denmark, Aalborg, Denmark. His research interests include power electronics and distributed energy-storage systems.

Kun Yu (Member, IEEE) received the M.S. degree from the Changsha University of Science and Technology, Changsha, China, in 2014, the Ph.D. degree from the Huazhong University of Science and Technology, Wuhan, in 2017, both in electrical engineering.

He is an Assistant Professor with the School of Electrical and Information Engineering, Changsha University of Science and Technology. His research interests include power system protection and control.

Chao Zhuo received the M.S. degree from the Changsha University of Science and Technology, Changsha, China, in 2011 and the Ph.D. degree from the Guangxi University, Nanning, in 2020, both in electrical engineering.

He is currently a Postdoctoral Fellow with the Changsha University of Science and Technology. His research interests include power system protection.